Beyond Photobleaching, Laser Illumination Unbinds Fluorescent Proteins

Katrin G. Heinze,*,† Santiago Costantino,† Paul De Koninck,‡ and Paul W. Wiseman§

Department of Physics and Department of Chemistry, McGill University, Montreal, Quebec, Canada, and Département de Biochimie et de Microbiologie, Université Laval, and Centre de Recherche Université Laval Robert-Giffard, Québec, Canada

Received: July 8, 2008; Revised Manuscript Received: November 18, 2008

Confocal and two-photon fluorescence microscopy techniques using genetically encoded fluorescent probes are widely used in cell biology. Beyond the common problems of photobleaching and phototoxicity, we present evidence that photounbinding also has the potential to compromise such methods, especially in quantitative studies. We show that laser intensities within excitation regimes typical for imaging approaches such as as fluorescence recovery after photobleaching (FRAP), photolysis, or fluorescence correlation spectroscopy (FCS) experiments can cause the dissociation of antibodies from their ligands. Indeed, both one- and two-photon excitation of a fluorescent anti-GFP antibody caused its dissociation from immobilized GFP in vitro. Importantly, with two-photon excitation, the laser intensity threshold for photobleaching was the same as for photounbinding. By contrast, with single-photon excitation, we found a range of laser intensities where photobleaching can be separated from photounbinding. This photounbinding effect was visualized and measured by rebinding a second fluorescent anti-GFP (Green Fluorescent Protein) antibody, indicating that the GFP remained functional for reassociation following the photoinduced dissociation. Finally, we show that this unbinding effect occurs only when at least one binding partner carries a fluorescent label. Our results show that this photounbinding effect can readily remain masked or be misinterpreted as photobleaching, which can compromise the quantitative interpretation of binding studies made using fluorescence microscopy.

Introduction

Laser illumination is widely used in confocal and two-photon (2P) fluorescence techniques for quantitative measurements of biological and biochemical processes. Despite many efforts to minimize the invasiveness of fluorescence approaches (e.g., reducing phototoxicity and photobleaching), it remains unclear as to how high or even moderate intensity light, restricted to a small volume,[1] can affect the local environment of the proteins or cellular structures under observation. In particular, for techniques using high laser intensities beyond the fluorescence saturation limit of the fluorophores, as in "fluorescence recovery after photobleaching" (FRAP) or "fluorescence loss in photobleaching" (FLIP), cell damage and phototoxicity effects have been demonstrated and recently quantified.[2]

Some of these photophysical effects have been successfully harnessed as fluorescence methods. For instance, "chromophore-assisted laser inactivation" (CALI) has been used as a photophysical method to assess the function of proteins in cells,[3] and photounbinding has been previously observed and used to study protein dynamics in neurons.[4] These methods rely on the fact that the absorption of intense laser light by fluorophores in close proximity can disrupt the natural conformation of proteins. However, the laser illumination conditions which can affect protein−protein interactions in the presence of bound fluorophores have never been systematically analyzed.

The impact of laser illumination within a small volume is particularly relevant for two-photon excitation (2PE) because (a) the required laser power for 2PE is approximately 1 order of magnitude higher than for one-photon excitation (1PE),[5] and (b) 2PE shows a square dependence on the excitation power, which narrows significantly the power range between fluorescence saturation and bleaching. Moreover, the high photon flux used for 2PE can potentially lead to higher-order photobleaching within the focal volume.[6] Thus, even though the risk of out-of focus bleaching is virtually eliminated in 2PE, bleaching within the focal volume is in fact much more problematic with 2PE in comparison with 1PE.[7]

In some fluorescence applications, photobleaching effects may overlap with photounbinding, making it difficult to discriminate between the two processes. In this study, we examine the photounbinding effect of laser illumination and make an attempt to discriminate photounbinding from photobleaching. We set out to test, under controlled conditions, whether laser illumination in either one or two-photon excitation modes leads to photounbinding of labeled proteins. We designed an in vitro system, based on antibody−antigen interactions using standard fluorescently tagged antibodies and GFP, to measure the photounbinding effects of laser illumination for power ranges typically employed in fluorescence imaging, photobleaching and photoactivation. Antibody−antigen binding is highly specific and reversible as it is mediated via noncovalent hydrogen, electrostatic, hydrophobic bonds and Van der Waals forces. Using these tools, we show that laser illumination leads to photounbinding in addition to photobleaching. Our results suggest that a significant amount of laser induced-protein dissociation can take place during standard fluorescence imaging experiments, potentially compromising the interpretation of imaging results.

Materials and Methods

Antibodies and Reagents. Three different antigen/antibody assays were used for this study.

* Corresponding author. E-mail: Katrin.heinze@imp.ac.at.
† Department of Physics, McGill University.
‡ Université Laval.
§ Department of Chemistry, McGill University.

10.1021/jp8060152 CCC: $40.75
Published on Web 03/23/2009

Assay 2F-GFP. This assay consisted of recombinant GFP and a monoclonal anti-GFP antibody labeled with different fluorophores (unlabeled (Pierce, Rockford, IL)), labeled with Alexa546 or Alexa647 (Invitrogen Canada Inc., Burlington, ON). Initially, one of the fluorescent anti-GFP antibodies was used to bind GFP, which was already cross-linked to the glass surface, and this sample was subsequently exposed to focused laser light of variable set intensities to induce (or not) photounbinding. Following laser illumination, the sample was incubated with an anti-GFP antibody tagged with a different fluorophore in order to reveal any rebinding after photounbinding. Confocal fluorescence imaging was used to monitor the samples at each step in order to visualize and measure the binding/rebinding process.

Assay 1F-GFP. This assay is similar to assay 2F-GFP, except that the anti-GFP antibody initially bound to GFP was not fluorescently labeled.

Assay nF-PDGFR. This assay was introduced to test photounbinding on an all-nonfluorescent assay (which can be turned into a fluorescent one using the same binding partners). This assay consisted of monoclonal antiplatelet derived growth factor receptor (PDGFR) β-antibody produced in mouse (isotope IgG 2b, stock solution: 4.3 mg IgG /mL, Sigma-Aldrich, Inc. Cat.No. P7679, St. Louis, MO), which served as the antigen in this assay and was immobilized onto the glass as described below. To allow optional fluorescent labeling, the antibody used was a biotin conjugated goat antimouse IgG2b (Fc specific) antibody (stock solution: 1.3 mg/mL, Pierce, Cat.No. 31805, Rockford, IL) to be labeled via a streptavidin system (AnaSpec, San Jose, CA) and biotin-conjugated fluorescein (AnaSpec). This served as a positive control, by turning this nF-PDGFR assay into the equivalent of a 1F-GFP assay, without changing the binding partners. We used the red fluorescent Alexa633 antimouse IgG2b antibody (stock solution: 2 mg/mL, dye to protein molar ratio: 2, Molecular Probes, Cat. No. A-21146, Eugene, OR) as a complementary secondary antibody to visualize potential rebinding for assay nF.

Immobilization Strategy. For this study, GFP (Assay 1F-GFP, 2F-GFP) or PDGFR IgG (assay nF-PDGFR) molecules were immobilized on glass substrates. Recombinant GFP or purified PDGF antibody were covalently bound to a coverslip by silanization (following the protocol recommended by Pierce, product no. 21650). This specific aminosilane reagent (Pierce) for immobilization also provided a spacer arm with a length of 16 Å to minimize surface effects on the protein−protein interactions.

Before immobilization, standard coverslips (Fisher Scientific, Nepean, ON) were cleaned with acetone (Sigma-Aldrich, Oakville, ON) and immersed in an acetone solution containing the amino-silane reagent (3-aminopropyltriethoxysilane, Pierce) for 60 s. The dried coverslips were assembled in custom-built glass-bottom dishes. Comparable commercially available glass-bottom culture dishes could not be used since the plastic parts do not tolerate the required acetone treatment.

For the cross-linking (immobilization) step, GFP or PDGFR antibody was diluted in PBS-EDTA (50 mM phosphate, 0.15 M NaCl, 10 mM EDTA, pH 7.2) and a 0.05 mg/mL GFP or PDGFR antibody solution incubated overnight at 4 °C in the glass bottom dish. Then, the dishes were rinsed thoroughly with PBS-EDTA to remove excessive cross-linker and then blocked with 2% BSA in PBS-EDTA for 20 min at RT. Antibodies against GFP were diluted to 0.25 mg/mL in PBS-EDTA containing 1% BSA and incubated in the same dish for 4 h at 4 °C. Finally, the GFP or PDGFR antibody-coated coverglass chamber was rinsed thoroughly and filled with PBS-EDTA solution. Proper coating was verified by fluorescence imaging.

For the all-nonfluorescent assay nF-PDGFR, a fluorescent grid structure was drawn on the respective coverglass by a lithographic process[8] before immobilization and assembly in dishes. This fluorescent fiduciary grid allowed for proper laser alignment for the unbinding experiment and precise post localization of the illuminated area by fluorescence imaging even in case of a negative rebinding result (no fluorescence from the labeled sample).

Control measurements were performed by blocking the silylated glass surface with 2% BSA in PBS-EDTA before cross-linking GFP or Alexa546-anti-GFP antibodies. In each case, only 2−5% of the original fluorescence was detected on the surface when this cross-linking was performed after the BSA treatment, indicating that the blocking step is sufficient to prevent nonspecific binding of the proteins to the silylated surface (Supporting Information Figure S1).

Photounbinding Setup. For the unbinding experiments, we used two independent setups (standard laser scanning microscope [LSM] and a custom assembled one) operating in one- and two-photon excitation modes. The first system was a commercial LSM setup (model FV300, Olympus Canada, ON) modified to provide options for one- or two-photon excitation (1PE or 2PE). To induce photobleaching and/or photounbinding, the laser (633 nm for 1PE or 800 nm for 2PE (Tsunami, Spectra Physics, Mountain View, CA, 200 fs pulses) was focused onto the antibody−antigen coated cover glass surface through the objective lens (UPlanApo-IR, 60×, 1.2 NA, Olympus Canada, ON) and raster scanned sequentially with 5.2 ms/line or 5.7 mm/s ("slow scan") to illuminate square subareas of 30 μm edge lengths with different laser powers. For this model of objective lens, and slightly overfilling the back aperture, the approximate size of the point-spread function (focal spot size) is approximately 0.5 fL, respectively; the full width at half-maximum (fwhm) is approximately 800 nm as determined in previous studies[9,18] by FCS experiments. For visualization and measurement of the bleaching/unbinding/rebinding effect, 1PE fluorescence imaging of the samples was performed in the same setup scanning with twice the speed (11.6 mm/s) using laser intensities which were an order of magnitude below the typical fluorescence saturation limits of the dyes used in order to avoid repeated photounbinding. In all cases, the laser power was measured before entering the back pupil of the objective lens and the transmission of the objective lens at 800 nm (information provided by Olympus) was taken into account. Thus, the reported power and/or intensity values are for the position "at the sample". Imaging was performed in three detection channels (green [GFP], yellow [Alexa546], red [Alexa633]). Excitation of GFP (and fluorescein) was provided by the 488 nm line of an Ar ion laser, excitation of Alexa546 by a 543 nm line of a HeNe laser, and excitation of Alexa647 by a 633 nm HeNe laser line, respectively. Emission from all fluorophores was collected with the same objective lens described above. The resulting fluorescence was split with a 570 nm dichroic mirror, and green fluorescence (GFP, fluorescein) were selected using BA510IF and BA530RIF emission filters (Chroma, Rockingham, VT) and detected with an internal PMT (type R3896, Hamamatsu, Japan). Longer wavelength emission was collected in a separate detection channel using a LP660 filter (Chroma Technology, Rockingham, VT). The laser powers and PMT voltages were adjusted and kept constant for all experiments such that no pixels were saturated in the image.

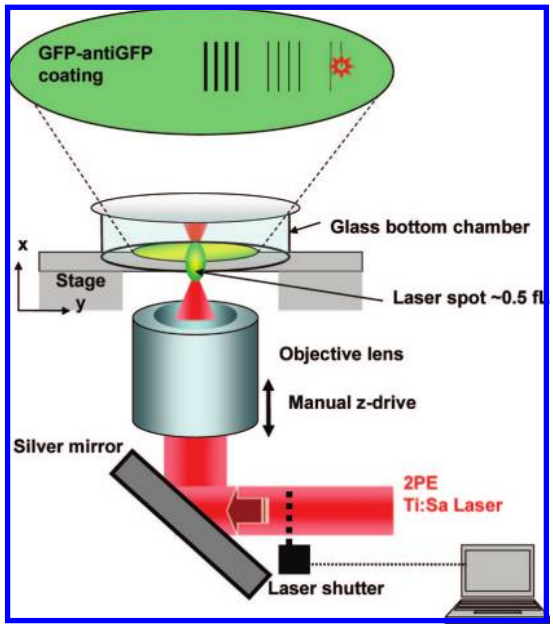

Figure 1. Principle of the custom-made illumination setup for inducing photobleaching and/or photounbinding. A pulsed femtosecond laser epi-illuminates a high-NA objective creating a diffraction limited spot. By moving the sample, the laser spot is scanned in lines (grouped according to the different intensities, top panel) along the coverglass surface on which the GFP and fluorescent anti-GFP complex is immobilized. Laser illumination creates photobleaching and/or photounbinding of the fluorescent antibody. The photounbinding effect can be indirectly measured by reincubation of the sample with a differently labeled anti-GFP antibody followed by fluorescence imaging in a standard LSM setup (setup not shown).

The second system permitted scanning the samples at lower speeds. Note, the custom-made setup (Figure 1) is only used for illumination, since it has no detectors, and only operated in two-photon excitation mode. A stationary Ti:Sa laser (emission at 800 nm, 200 fs pulse width, 80 MHz repetition rate) epi-illuminates an objective lens (s.a.) similar to an inverted micrsoscope setup. The size of the focal spot is approximately the same as that for the commercial LSM setup (0.5 fL) as we use the same objective lens, laser settings, and laser beam diameter coupled into the objective lens. A motorized stage (Thorlabs, Newton, NJ)[7] was used to move the sample during laser illumination to generate line scans. A PC with custom-written LabVIEW 7.0 (National Instruments, Austin, TX) programs and drivers controlled a mechanical shutter (Newport, Mountain View, CA) which varied the exposure of the surface to laser illumination during the scan. Precise positioning of the laser focus on the coverslip surface was accomplished by monitoring the intensity of the back-reflection off the glass in a confocal setup. To induce photobleaching and/or photounbinding, the laser was focused onto the GFP/anti-GFP-coated cover glass surface and scanned to generate sequential square illumination patterns of four parallel lines, with each pattern of lines scanned at a different laser power (see Figure 2). The laser power was varied from 7 to 56 mW for each separate pattern of 4 lines scanned on the sample surface, starting with the highest power in the lower left corner of the image and the lowest in the upper right corner (Figure 2). The laser power schematic diagram is shown in Figure 2 (panel B2). All lines were traced with a constant scan velocity of 40 μm/s or 500 ms/line.

Photounbinding Data Acquisition. The experiment involves a four-step procedure: (1) illumination of the antigen−antibody-coating to induce photounbinding, (2) acquisition of a fluorescence image of the illuminated area, (3) reincubation with a fluorescently labeled antibody tagged with a different fluorophore, and (4) aquisition of a second fluorescence image to visualize and measure specific rebinding and hence spatially resolve locations where photounbinding occurred as a function of laser power.

(1) The coverglass with the antigen−antibody complex was covered with 10 mL PBS-EDTA solution and illuminated in square patches using a standard LSM instrument or groups of scan lines (custom-built setup, Figure 1 as described above). If illumination causes photounbinding, the laser light dissociates the antibody from the antigen leaving the cross-linked antigen and a vacant binding site.

(2) A three-channel fluorescence image of the illuminated area was obtained. Green corresponds to GFP (assay 1F-GFP, 2F-GFP) or biotin conjugated fluorescein (assay nF-PDGFR); yellow corresponds to the Alexa546-anti-GFP (assay F), and red corresponds to the Alexa647-anti-GFP, (1F-GFP, 2F-GFP), Alexa633 antimouse IgG2b (assay nF-PDGFR), or Alexa647-phalloidin (Supporting Information, Figure S1).

(3) The sample was postincubated with an anti-GFP antibody tagged with a fluorophore of different emission wavelength (1F-GFP, 2F-GFP, Alexa546 or Alexa647) or an Alexa633 anti-mouse IgG2b (assay nF-PDGFR) to specifically relabel the vacant binding sites that became exposed due to photounbinding and to provide contrast against those sites still occupied by the original but photobleached fluorescently tagged antibody. Control images in the green channel are used to verify that the covalently linked GFP remains fluorescent on the glass and is not removed or photobleached by the laser illumination.

(4) A second fluorescence image was collected and compared with the original image taken before reincubation. Intensity measurements of the scanned patterns in the fluorescence images were used to quantify the degree of photounbinding/photobleaching as a function of laser power. The laser power for imaging was always kept 1 order of magnitude below the fluorescence saturation limit to avoid additional unbinding.

Results

To test whether the binding of fluorescent proteins is affected by laser illumination, we illuminated the immobilized fluorescent antibody-GFP antigen complex with various laser intensities. For these experiments, tested the photoinduced unbinding effect upon one- and two-photon excitation on either fluorescent or nonfluorescent probes. Figure 1 (top) shows a sketched outline of the laser-induced unbinding experiment. To assay the photounbinding, we reapplied the same antibody but with a different label on the immobilized sample and quantified the fluorescence intensity of the newly bound probe.

Control measurements to ensure the specificity of the (a) GFP binding to the cross-linker and (b) fluorescent GFP-antibody to GFP are described in Supporting Information.

Unbinding of a Fluorescent and a Nonfluorescent Antibody by Two-Photon Excitation. Illumination of fluorescently tagged (Alexa546; Figure 2A) or untagged anti-GFP antibody (Figure 2B) was performed in our custom-made illumination setup (Figure 1). As shown in the images in Figure 2, vertical lines were scanned on the coverglass with pulsed 800 nm laser light at various powers, from 7 to 56 mW (scan speed: 500 ms/line). The coordinates of each intensity pattern are shown in panel B2. Note, we indicate both the average laser power used and the total laser energy per area. In Supporting

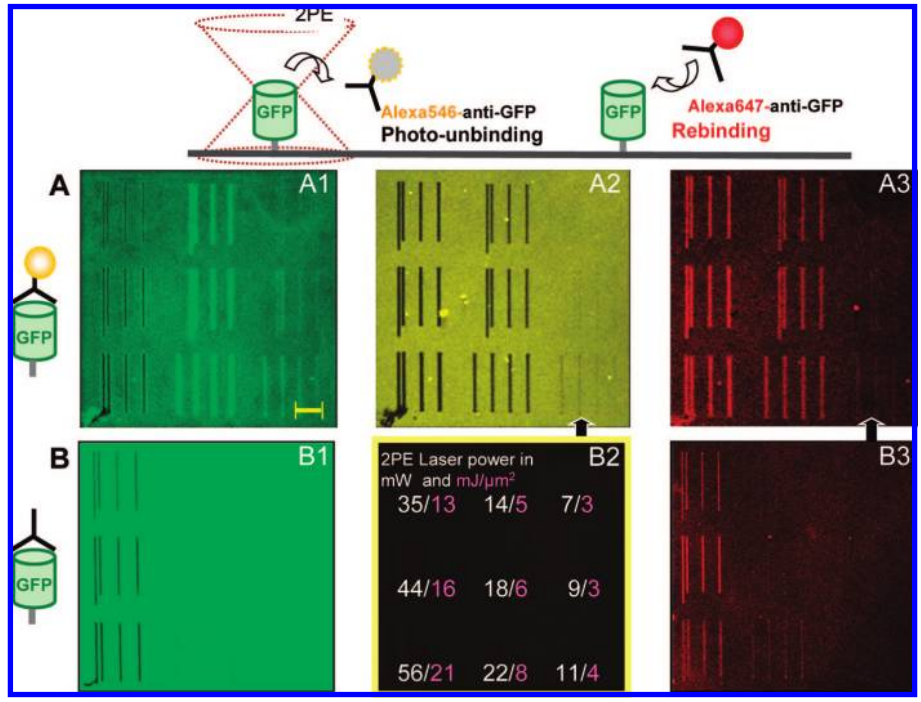

Figure 2. Photounbinding of fluorescent and nonfluorescent anti-GFP by two-photon excitation. The GFP/Alexa546-anti-GFP complex (A) or GFP/anti-GFP complex (B) was scanned with two-photon excitation in stripe patterns (laser powers in mW were varied as indicated panel B2) and subsequently incubated with Alexa647-anti-GFP and then imaged in three detection channels (1[GFP], 2[Alexa546], 3[Alexa647]) to measure rebinding of the antibody to GFP. In panel A1 (scale bar: 10 μm, scan speed for "drawing" the stripes: 500 ms/ stripe) the increase in GFP fluorescence inside the stripes for 9 to 22 mW correlates with the decrease in Alexa546 fluorescence (A2), suggesting a reduction of FRET between the GFP and the Alexa546 (which is not observable in the case of unlabeled anti-GFP (B1)). In A, the decrease in Alexa546 fluorescence with laser power (A2) is accompanied by an increase in Alexa647 fluorescence (A3), indicating an unbinding of Alexa546-anti-GFP from GFP caused by two-photon laser illumination. Rebinding of Alexa647-anti-GFP to GFP can be observed even in the case of minimal reduction in Alexa546 fluorescence (see black arrows in A2 and A3), indicating that even if photobleaching of Alexa546 occurred, it is indistinguishable from photounbinding. In B the rebinding of Alexa647-anti-GFP to GFP is detected only at laser powers >18 mW, suggesting that unbinding of unlabeled anti-GFP (B) from GFP requires more power than Alexa546-anti-GFP (A).

Information, we explain in detail how the total energy values were calculated.

To assay for any photoinduced unbinding of Alexa546-anti-GFP (panel A2) from GFP (panel A1) or unlabeled anti-GFP (panel B2) from GFP (panel B1), the slides were washed and incubated with Alexa647-anti-GFP (panel A3, B3). We then imaged the slides in three channels (1, green{488 nm}; 2, yellow{543 nm}; and 3, red{633 nm}) using a confocal microscope. The sketches indicate which molecular species and features were probed for each channel.

The confocal image in Figure 2, panel A2 demonstrates that laser illumination above 7 mW produced stripes in the Alexa546-anti-GFP layer, which became darker (i.e., less fluorescence) with increasing laser power. The standard interpretation for these results would be photobleaching of Alexa546. However, the predominant rebinding of Alexa647-anti-GFP antibody (red stripes in panel A3) to the same areas after the laser exposure shows that the binding sites have become accessible to the new antibody. Indeed, there is a strong correlation between the darkness of the stripes in panel A2 and the brightness of the red fluorescence at the same stripe locations in panel A3 indicating rebinding of Alexa647-anti-GFP antibody at the positions where the Alexa546-anti-GFP antibody has been removed as a result of laser light exposure. Figure 3B shows the good correlation between the disappearance of Alexa546 fluorescence (Figure 2, panel A2) and the increase in Alexa647 (Figure 2, panel A3) for eight independent measurements, consistent with a unbinding−rebinding sequence. These results indicate that two-photon laser illumination of fluorescently labeled antibodies above a certain threshold can lead to their photounbinding from their antigen. If laser illumination only induced photobleaching without unbinding, postincubation with the Alexa647-anti-GFP antibody would simply result in a diffuse homogeneous fluorescence (i.e., background nonspecific binding) instead of the site specific stripe patterns which are evident in Figure 2, panel A3.

A notewhorty additional effect of the unbinding of Alexa546 is the increase in GFP fluorescence (Figure 2, panel A1), which most likely arises from a reduction in Förster resonance energy transfer (FRET) or fluorescence quenching between the GFP and the Alexa546. These green stripes also confirm that (i) GFP itself remained attached to the substrate after laser exposure and (ii) the observed red stripes in panel C are in the same coordinates as the green stripes, consistent with a specific binding to GFP, and not the coverglass. In addition, contrary to its labeled antibody (Figure 2, panel A2), GFP (panel A1) was not photobleached below 35 mW, as the two-photon cross section to excite GFP at 800 nm is very low (absorption maximum at ~950 nm).[10,11] However, at higher laser intensities (35−56 mW), GFP did undergo some photobleaching but not photounbinding since the rebinding was even higher in panel A3. Figure 3A emphasizes the biphasic relationship between GFP and Alexa 546 fluorescence ($n = 8$) and reflects the transition from loss of FRET to GFP photobleaching (Figure 2, panel A1) as the laser power is increased and the Alexa 546 diminishes (panel A2).

To test whether the fluorescent label on the antibody was important for this photounbinding effect, we repeated a similar experiment, except that the anti-GFP was unlabeled (Figure 2, panel B). In this experiment, unbinding of the nonfluorescent

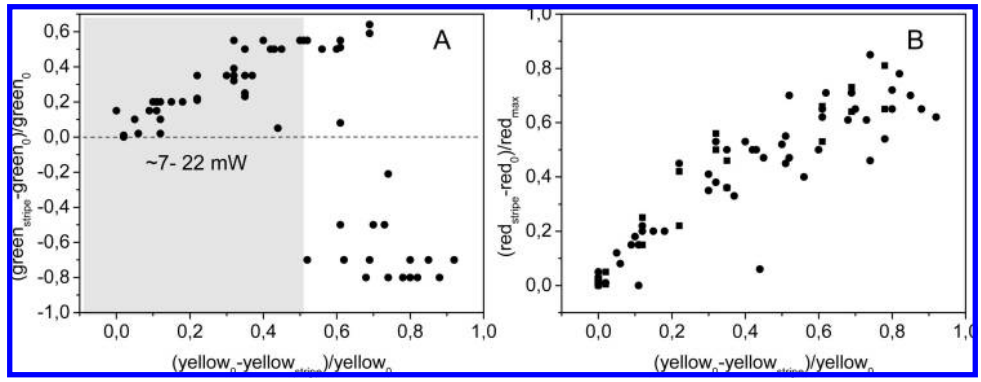

Figure 3. Relationship between the loss of Alexa546 fluorescence (bleaching/unbinding) with the changes in GFP emission (A) and the increase in Alexa 647 fluorescence (rebinding) (B) over a wide range of laser powers ($n = 8$). A: The biphasic relationship between GFP and Alexa 546 fluorescence reveals a loss of FRET (increased GFP emission upon Alexa546 bleaching/unbinding) at laser powers between 7 and 22 mW (gray area), followed by photodestruction of GFP at laser power ≥ 35 mW. B: The red fluorescence of the rebinding antibody is monotonically increasing with loss of the originally bound anti-GFP.

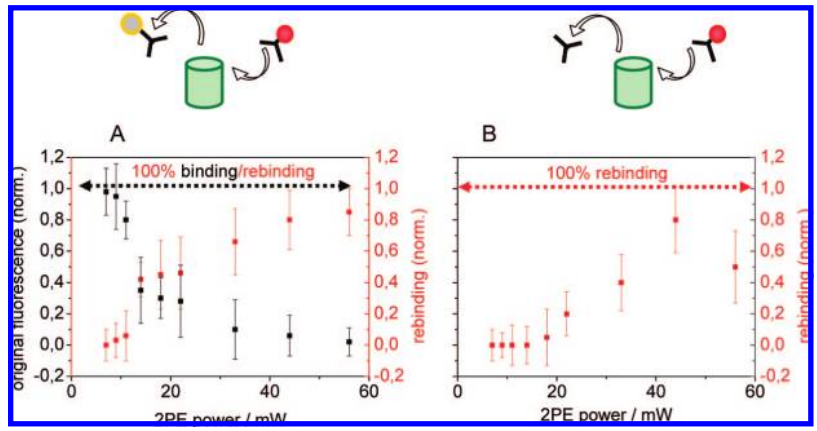

Figure 4. Relationship between laser power and photounbinding for fluorescent and nonfluorescent anti-GFP: The photounbinding effect is more pronounced for the strongly absorbing Alexa546-anti-GFP compared with the nonfluorescent anti-GFP. The graphs show the rebinding of Alexa647-anti-GFP (red squares) after increasing levels of laser power in the case of labeled (A) and unlabeled (B) anti-GFP. The measured fluorescent intensity of the Alexa647 antibody bound to GFP in a control experiment provided the 100% (set to a value of 1) value for the rebinding condition. Also shown in A is the inversely correlated unbinding of Alexa546 (black squares). Data represent mean ($n = 8$) values that were scaled (for rebinding) to maximum binding of Alexa647-anti-GFP to GFP without prior Alexa546-anti-GFP binding, or (for unbinding) to initial levels of Alexa546-anti-GFP before laser excitation.

antibody is assessed solely by the concommittent increase in Alexa647 (panel B3). Incidently, because no FRET loss occurs in this case, the unbinding of a nonfluorescent anti-GFP antibody did not lead to increase GFP fluorescence (as it was seen in panel A3). Panel B3 shows that despite the absence of an Alexa dye on the GFP antibody, laser illumination caused a significant unbinding of the antibody, albeit at higher laser powers (≥22 mW). The following two possibility might account for this high laser power-induced unbinding of nonfluorescent antibody: (1) light absorption by the nonfluorescent antibody is sufficient to disrupt binding and (2) the antigen GFP absorbed sufficient light at 800 nm[10,11] to destabilize the interaction with the antibody. The fact that unbinding of the nonfluorescent antibody was detectable at laser intensities matching those that caused GFP photobleaching (compare panel B1 and B3 in Figure 2) is consistent with the latter interpretation.

Figure 4 directly compares photounbinding of a labeled (Figure 2A) versus unlabeled (Figure 2B) antibody by plotting the fluorescence intensity of Alexa647 after rebinding as a function of laser power. For calibration, we performed a separate experiment in which we applied the Alexa647-labeled antibody directly (without previous illumination) to the immobilized GFP. Our results indicate that rebinding of Alexa647-anti-GFP after laser illumination reached up to 85% and 70% (relative to the calibration control, see Figure 4 legend) following photounbinding of the Alexa546 labeled (Figure 4A) and unlabeled (Figure 4B) antibodies, respectively. Assuming a rebinding/unbinding ratio of 1:1 and linearity of emission, we conclude that these relative fluorescence levels are proportional to the number of antibody molecules that were previously unbound by the laser illumination. The trial-to-trial error was ±30% mainly due to technical difficulties in ensuring a submicrometer exact alignment of the illumination plane.

Absence of Photounbinding of a Nonfluorescent Antibody from Its Nonfluorescent Antigen after Two-Photon Illumination. To test whether light absorption by a nonfluorescent antibody is capable of disrupting binding to its antigen, we exposed an unlabeled antibody bound to a nonfluorescent antigen to two-photon illumination. For these experiments, we chose to use a primary−secondary antibody combination. The primary antibody from mouse (directed against PDGF-receptor β) served as the antigen for the secondary antibody and was absorbed onto the coverglass in the same manner as the GFP in Figure 2. A biotinylated-goat antimouse secondary antibody was then used for binding to the primary antibody. One major problem with this approach is that the sample is completely nonfluorescent, hampering proper focusing on the sample as well as retrieval of the illuminated areas. We thus modified our

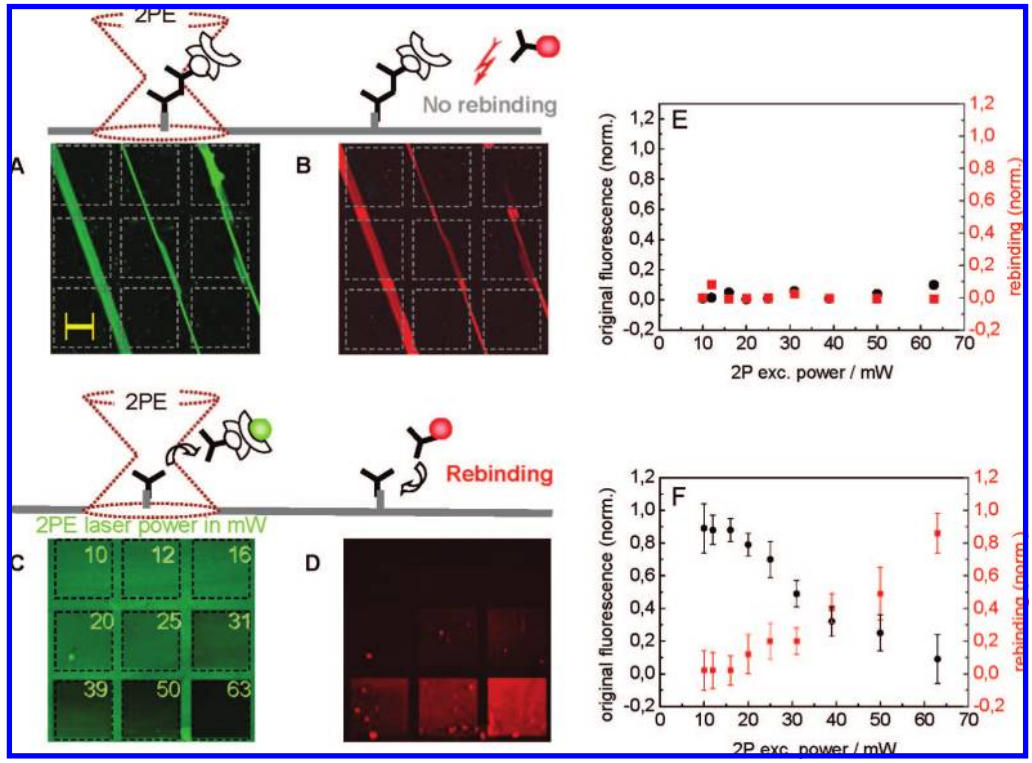

Figure 5. Lack of detectable photounbinding of nonfluorescent antigen from nonfluorescent antibody. A complex of anti-PDGF-receptor β/biotinylated-IgG2b antibody was scanned with two-photon excitation in square patterns using a standard LSM setup (laser intensities in mW were varied as indicated in E) and subsequently incubated with Alexa633-IgG2b antibody and then imaged in two detection channels (A[green], scale bar: 15 μm, B[Alexa633]). The diagonal fluorescent lines visible in both A and B were patterned on the glass by a custom lithographic method (see text and Costantino et al., 2005) as a fiduciary grid for recognizing and relocating the illuminated areas of interest within the field of view, since nonfluorescent binding partners were used in this assay. In B, the photobleached segments of the grid allow identification of the illuminated square patterns, which are indicated by the dashed lines. No rebinding was detected (B). C,D: As a positive control, the same complex was labeled via streptavidin/biotin conjugated with fluorescein. (C) Laser powers >16 mW caused photounbinding of the fluorescent secondary antibody from the anti-PDGF receptor antibody, as confirmed by the binding of Alexa633-anti-IgG2b (D). The scan speed to "draw" the squares was kept constant at 5.2 ms/line. The loss of fluorescence and rebinding observed in experiment A,B and C,D is plotted in E and F, respectively.

coverslips by creating a fluorescent fiduciary grid directly on the glass surface using a laser-based lithographic technique that we developed previously[8] and used the (bleached) grid fluorescence as a marker to identify the original pattern of illumination (Figure 5A,B). Briefly, the grid consists of a pattern of stripes of resin containing multiple fluorescent agents cured by two-photon excitation on the coverglass. Note that only the red fluorescence was photobleached (the green fluorescence being less susceptible to 2PE at 800 nm). Using this method, we were able to achieve proper focusing of the laser on the sample and relocate the areas exposed to laser illumination. For these experiments, we used a standard LSM to scan (5.2 ms/line) the focus of a femtosecond laser beam across square regions on the sample while varying the laser power between 10−63 mW. After the illumination procedure, another secondary antibody (goat antimouse) tagged with Alexa633 was applied on the sample. By matching the fluorescence from the fiduciary grid in the green and red channels, it was possible to relocate the square areas on the glass substrate that had been illuminated. The results showed no rebinding of the second Alexa633-antibody, suggesting that the laser illumination had no impact on the binding between the nonfluorescent primary and secondary antibodies.

To confirm that there was truly a primary/secondary antibody complex on the coverglass, we probed the biotinylated secondary antibody with a two-step binding of streptavidin and biotin conjugated with fluorescein (green). The green fluorescence seen in Figure 5C indeed clearly indicates that the complex was there. Furthermore, when we then exposed this fluorescent sample to increasing amounts of laser power, we found that it caused a significant unbinding of the fluorescent complex at $\geq$20 mW (Figure 5C), as shown by the rebinding of Alexa633-goat antimouse antibody (Figure 5D). This positive control experiment confirms that the binding partners used for the nonfluorescent assay could be separated by laser light, but only if one partner carried a fluorescent tag. We note that for this control experiment, it was not necessary to include a fiduciary grid, as the sample was fluorescent; however, we repeated this control in presence of the grid and observed the same results (not shown). Quantification of the described results concerning loss of fluorescence and rebinding dependend on laser power is given in Figure 5E (nonfluorescent assay) and Figure 5F (positive control).

Photounbinding by Two-Photon versus One-Photon Illumination. The above results indicate that two-photon absorption of fluorescently labeled proteins can lead to photounbinding. We designed an experiment to compare the photounbinding effect of one versus two-photon excitation using the standard LSM and the same GFP/anti-GFP antibody strategy, except that we swaped the two differently labeled anti-GFPs, now using the red (Alexa647) one for the initial binding and the orange (Alexa546) one for the rebinding step. With one photon excitation (at 633 nm), laser powers $\geq$23 μW caused significant reduction in the fluorescence as seen in the dark squares in Figure 6A (the respective laser power/energy used is indicated in the bottom panels labeld with 1PE and 2PE respectively).

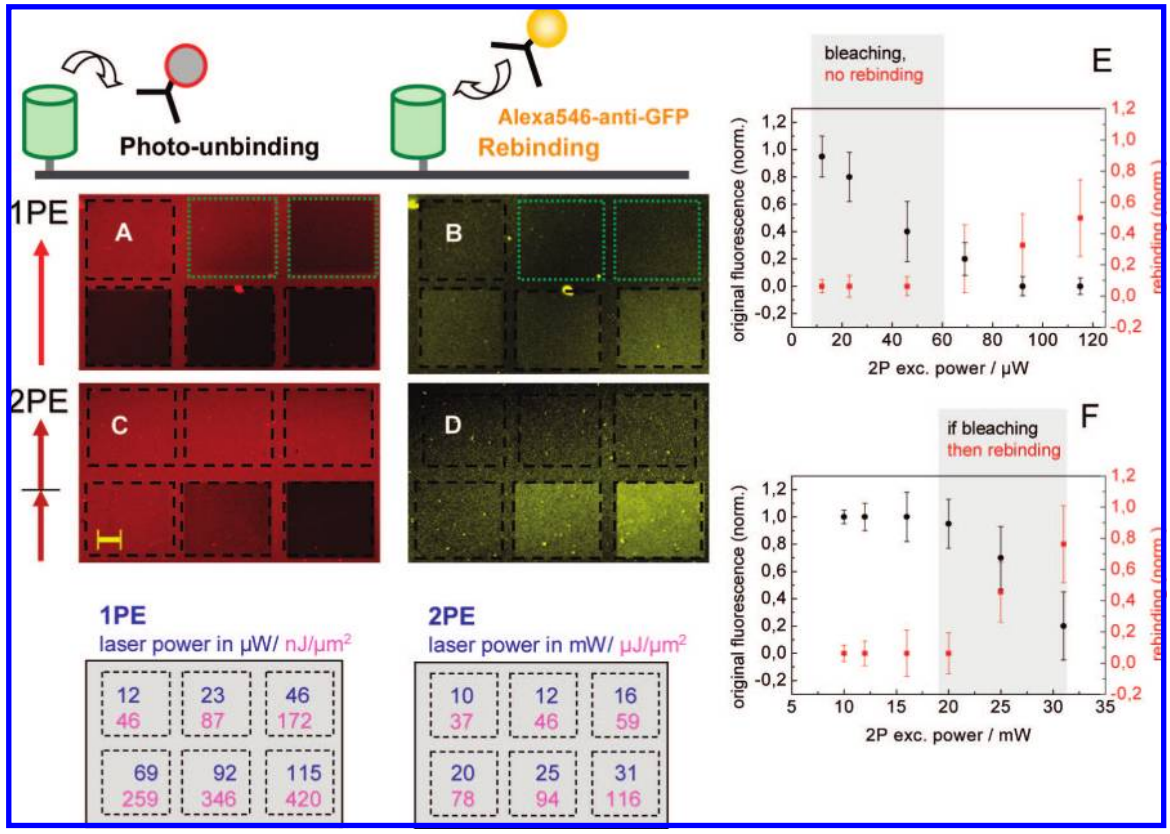

Figure 6. Photounbinding caused by one-photon versus two-photon excitation. A complex of GFP/Alexa647-anti-GFP was scanned with either one-photon (633 nm, A,B) or two-photon (830 nm, C,D) excitation in square patterns using a standard LSM setup (laser intensities in mW were varied as indicated in the bottom panels, scan speed as in Figure 5) and subsequently incubated with Alexa546-anti-GFP antibody and then imaged in two detection channels (A, C[Alexa647], B, D[Alexa546]). Scale bar: 10 μm. Photounbinding of Alexa647-anti-GFP from GFP (A,C) occurs under both 1PE and 2PE, as confirmed by the rebinding of Alexa546-anti-GFP (B,D). The green dotted squares highlight a laser power window where one-photon excitation caused mainly photobleaching with little, if any, photounbinding. In contrast, with two-photon excitation, no window of laser power allows for the separation of photobleaching from photounbinding. In the graphs (E) and 2PE (F), this power window is highlighted in gray. The photounbinding effect is stronger in case of 2PE (up to 80% unbinding versus 50% for 1PE).

However, in this case, part of this reduction cannot be accounted by photounbinding. Indeed, the yellow squares in Figure 6B show an increase in fluorescence only $\geq$69 μW, suggesting that there is a "window" of laser powers (in this case 23−46 μW; highlighted by the dotted green frames in Figure 6 A,B) that can cause photobleaching without photounbinding. The respective graph (Figure 6E) shows the loss of fluorescence and rebinding and indicates the power range where photobleaching occurs without rebinding (highlighted in gray). In contrast, with two-photon excitation, we could not resolve such a "window" of laser power separating photobleaching from photounbinding (Figure 6F, highlighted in gray). Indeed, as shown in Figure 2, Figure 5C,D, and Figure 6C,D with the same antibody configuration as used for the one photon experiment, the disappearance of fluorescence from the first antibody always correlates with the appearance of new fluorescence from the binding of the second antibody.

Discussion

We have demonstrated that one- or two-photon laser illumination for LSM can significantly disrupt antigen−antibody dissociation constants if a fluorescent label is involved. As compared with one-photon excitation, the effect of photounbinding is more pronounced after two-photon excitation where we could not resolve a clear threshold in laser power where we observed only photobleaching with no simultaneous photounbinding. The central point of this study is that laser illumination can alter the antigen−antibody binding reaction, leading to possible underestimation of binding constants or overestimation of dissociation constants.

In our experiments, we varied the laser power in order to cover ranges that have been reported for two-photon applications, such as FCS (up to 20 mW [9,13]) and FRAP (100 mW,[15] and 35−65 mW [16]), as well as photolysis of caged compounds (up to 11 mW [17]).

The assay that we have designed for this study allowed us to reveal not only the photounbinding effect of laser illumination but also the safe window, if any, where photobleaching can be discriminated from photounbinding. The key in our experiments is that a vacated binding site after photounbinding is made available for rebinding, whereas a binding site occupied by a molecule carrying a bleached fluorophore is not. On the other hand, this assay cannot measure with high precision the photounbinding effect, because it uses a confocal configurationon a very thin surface (coverglass), which can be uneven, bent, or tilted. Nevertheless, our study clearly shows that photounbinding may be present "incognito" under common fluorescence experimental conditions. Moreover, unless similar photounbinding measurements are performed, an unwary experimenter might misinterpret the disappearance of fluorescence as photobleaching only. This problem would, for instance, be particularly problematic for quantitative fluorescence-based binding studies. For example, for FRAP applications, it is assumed that the molecular species observed and their bio-

chemical environments are "equivalent" inside and outside the bleached region. The measured recovery in fluorescence is assumed to be due to mobile fluorescent species outside of the bleached region, and the plateau is assumed to be due to immobile photobleached species inside the region. However, if proteins are also photounbound, these assumptions are no longer valid as the binding equilibrium has been changed by light exposure within the bleached region. The observed kinetics of recovery will then reflect both rebinding of fluorescent labels and diffusive transport into the region, and the measured immobile fraction will also have a systematic error.

For FCS studies, the photounbinding would introduce different artifacts. In these experiments, binding is usually determined by (a) a change in the diffusion time using single color FCS in the autocorrelation mode or (b) coincident fluctuations in two spectrally distinct detection channels using dual color FCCS (cross-correlation mode). For FCS, binding will simply be underestimated as the induced unbinding effectively appears as an increased mobility of the proteins. For FCCS, the amplitude of the cross-correlation function will decrease substantially because of the dissociation of the original binding partners and because a pool of bleached "free" binding partners can then immediately rebind to a fluorescently labeled partner, but the binding and formation of such a complex would not be detected by FCCS because of the missing second color.

Pinpointing and associating imaging artifacts to a specific source of bias is challenging because of the power thresholds for the onset of bleaching and photounbinding are close (1P) or not resolvable in our study (2P). The best strategy to minimize this bias is to stay significantly below the bleaching threshold; however, this is not trivial to determine for two-photon excitation as has been shown recently.[19] Of course, for FRAP, which is based on photobleaching, such artifacts may not be entirely avoidable, particurlaly for two-photon FRAP. Unfortunately, even performing a bleaching intensity series to determine an intensity level below which the fluorescence recovery does not significantly change would not necessarily be a reliable indicator of unbiased data. By imaging Ca^{2+} transients in neurons using 2PE, Hopt and Neher and others[20] have shown that there are very early signs of photodamage that are underestimated when looking only at fluorescence photobleaching, and these become more enhanced for shorter laser pulses.

Our results suggest that this effect is fluorescent label-dependent and most likely primarily dependent on the absorption cross sections of the fluorophores used. Importantly, there is evidence from the previous study by Akaaboune et al. (2002) that photounbinding is neither induced by surface effects nor limited to in vitro applications. Our findings are in fact consistent with the results described by Akaaboune and co-workers. Of course, absolute values, such as power levels, are dependent on the photostability or saturation limits of the individual label used as well as the scanning conditions.

The photophysical mechanism of fluorophore photounbinding is not well-understood. Nonspecific thermal effects within the focal volume are highly unlikely, because in vitro experiments performed previously suggested that the very weak photon absorption of water, which corresponds to the first order cross section for water at 720−800 nm,[1,21] would lead to a negligible increase in temperature. We estimate that, under our experimental conditions, laser powers beyond the bleaching threshold would result in a temperature increase in the focal volume of less than 2 K. Furthermore, we observed photounbinding only for fluorescently labeled samples; in case of a nonspecific thermal effect, we would expect to observe the same photounbinding for an unlabeled antibody/antigen system. However, we cannot exclude a label specific heat effect or "label induced" thermo-optic effect as it can be observed in plants, where pigment arrays can undergo substantial structural rearrangements (e.g., trimer to monomer transitions) after exposure to light.[22] The photophysical mechanisms responsible for the observed unbinding phenomenon may also be related to photoionization mechanisms, as have been characterized in laser dissection.[23] However, the laser intensities reported to induce laser ablation of biological material with femtosecond lasers were 20% higher than the threshold for photobleaching,[24] which contrasts with our observations that no clear window of laser power could separate photobleaching from photounbinding. Alternatively, photounbinding may be induced by oxygen-derived radicals that are common in biological systems[3] and can be produced during fluorescence microscopy and spectroscopy measurements. Laser excitation may also cause perturbations in protein vibration,[25] or conformational changes of the proteins involved as originally suggested by Aakaboune and co-workers.[4] Metastable states or higher excitation levels of the fluorophore after intense laser illumination may be involved: the "stored" (absorbed) light energy could be partly transferred to the protein resulting in conformational changes and therefore dramatic shifts in the binding affinities. In any case, the mechanism of photounbinding appears distinct from that of photobleaching, because of the differences we observe between 1PE and 2PE.

Laser-induced photounbinding will likely depend on the specific sample preparation and fluorophores used, but it is important to stress that we observed antibody unbinding with commonly used fluorophores (GFP, antibodies labeled with Alexa dyes) and standard laser powers.[1,9,14−18]

Previous studies of others[4] as well as preliminary photounbinding studies in our laboratory on calmodulin and calmodulin-binding peptides strongly suggest that photounbinding is not a peculiarity of the assays presented and not restricted to antigen−antibody pairs. Currently, we are interested in whether photounbinding depends on the dissociation constants for the pair of proteins under study. As there have been a large number of quantitative studies performed in the past decade based on laser illumination of fluorescent probes, our findings suggest that photounbinding may need to be considered in their interpretation.

Acknowledgment. We thank Dr. Petra Schwille for valuable discussions, Dr. M. Neal Waxham for providing helpful suggestions, and Dr. Gyözö Garab for discussions about potential mechanisms of the observed photounbinding effect. We thank Drs. K. Elsayad and A. Godin for assistance in the evaluation of the local and total incident laser energy. Research was funded by the Natural Science and Engineering Research Council of Canada (P.W.W. and P.D.K.), the Canadian Foundation for Innovation (P.W.W. and P.D.K.), and Human Frontier Science Program (P.D.K. and P.W.W.). P.D.K. was supported by a Career Award from the Canadian Institute for Health Research (CIHR); S.C. and K.G.H. were supported by the Neurophysics CIHR Strategic Training Program Grant.

Supporting Information Available: Figure S1: Controls show that BSA coating is sufficient to prevent nonspecific binding (control 1) and that rebinding occurs exclusively for antibodies specific to its target (control 2). Figure S2 and S3, laser intensity evaluation. Figure S2: Sketch of incident laser beam, to explain the calculations of the local and total incident energy for various scan modes. The sketch shows the cylindrical coordinate axes used. Figure S3: Scheme of the laser beam path

using the "normal scan mode" in a LSM (height of scan lines $= L_1$, width of scan lines $= L_2$) as a series of parallel lines separated by a (center−center) distance a. This information is available free of charge via the Internet at http://pubs.acs.org.

References and Notes

(1) Denk, W.; Piston, D.; Webb, W. W. In *Handbook of Confocal Microscopy*; Pawley, J. B., Ed.; Plenum Press, New York., 1995; p 445.
(2) Dobrucki, J. W.; Feret, D.; Noatynska, A. *Biophys. J.* **2007**, *93*, 1778.
(3) Tanabe, T.; Oyamada, M.; Fujita, K.; Dai, P; Tanaka, H.; Takamatsu, T. *Nat. Methods* **2005**, *2*, 503.
(4) Akaaboune, M.; Grady, R. M.; Turney, S.; Sanes, J. R.; Lichtman, J. W. *Neuron* **2002**, *34*, 865.
(5) Kim, S. A.; Heinze, K. G.; Schwille, P. *Nat. Methods* **2007**, *4*, 963.
(6) Chen, T.-S.; Zeng, S.-Q.; Luo, Q.-M.; Zhang, Z.-H.; Zhou, W. *Biochem. Biophys. Res. Commun.* **2002**, *291*, 1275.
(7) Patterson, G. H.; Piston, D. W. *Biophys. J.* **2000**, *78*, 2159.
(8) Costantino, S.; Heinze, K. G.; Martinez, O. E.; De Koninck, P.; Wiseman, P. W. *Microsc. Res. Tech.* **2005**, *68*, 272.
(9) Kohl, T.; Heinze, K. G.; Kuhlemann, R.; Koltermann, A.; Schwille, P. *Proc. Natl. Acad. Sci. U.S.A.* **2002**, *99*, 12161.
(10) Zipfel, W. R.; Williams, R. M.; Webb, W. W. *Nat. Biotechnol.* **2003**, *21*, 1369.
(11) Blab, G. A.; Lommerse, P. H. M.; Cognet, L.; Harms, G. S.; Schmidt, T. *Chem. Phys. Lett.* **2001**, *350*, 71.
(12) Bacia, K.; Majoul, I. V.; Schwille, P. *Biophys. J.* **2002**, *83*, 1184.
(13) Sprague, B. L.; Pego, R. L.; Stavreva, D. A.; McNally, J. G. *Biophys. J.* **2004**, *86*, 3473.
(14) Merkle, D.; Block, W. D.; Yu, Y.; Lees-Miller, S. P.; Cramb, D. T. *Biochemistry* **2006**, *45*, 4164.
(15) Basu, S.; Wolgemuth, C. W.; Campagnola, P. J. *Biomacromolecules* **2004**, *5*, 2347.
(16) Schmidt, H.; Arendt, O.; Brown, E. B.; Schwaller, B.; Eilers, J. *J. Neurochem.* **2007**, *100*, 727.
(17) Dakin, K.; Li, W. H. *Nat. Methods* **2006**, *12*, 959.
(18) Heinze, K. G.; Jahnz, M.; Schwille, P. *Biophys. J.* **2004**, *86*, 506.
(19) Wu, J.; Berland, K. *Microsc. Res. Tech.* **2007**, *70*, 682.
(20) Hopt, A.; Neher, E. *Biophys. J.* **2001**, *80* (4), 2029.
(21) Schönle, A.; Hell, S. W. *Opt. Lett.* **1998**, *23*, 325.
(22) Cseh, Z.; Rajagopal, S.; Tsonev, T.; Busheva, M.; Papp, E. G. *Biochemistry* **2000**, *39*, 15250.
(23) König, K.; Riemann, I.; Fritzsche, W. *Opt. Lett.* **2001**, *26*, 819.
(24) Heisterkamp, A.; Maxwell, I. Z.; Mazur, E.; Underwood, J. M.; Nickerson, J. A.; Kumar, S.; Ingber, D. E. *Opt. Express* **2005**, *13*, 3690.
(25) Haliloglu, T.; Keskin, O.; Ma, B.; Nussinov, R. *Biophys. J.* **2005**, *88*, 1552.

JP8060152